International Forum on Aeroelasticity and Structural Dynamics
IFASD 2017
25-28 June 2017, Como - Italy

LIMIT CYCLE OSCILLATION OF A SUPERSONIC TRANSPORT MODEL IN A TRANSONIC WIND TUNNEL TEST

Kenichi SAITOH [1], Norio YOSHIMOTO [2], and Hamidreza KHEIRANDISH [3]

[1, 2] Japan Aerospace Exploration Agency
Tokyo, Japan
[1] saitoh.kenichi@jaxa.jp
[2] yoshimoto.norio@jaxa.jp

[3] Advanced Science & Intelligence Research Institute
Tokyo, Japan
hamidkh@asiri.co.jp

Keywords: LCO, Supersonic Transport, Wind tunnel test, Transonic flow.

Abstract: Aeroelastic characteristics of Supersonic Transport (SST) was investigated in wind tunnel test. Amplitude variation of Limit Cycle Oscillation (LCO) with respect to Mach number and dynamic pressure was measured in the wind tunnel experiment. The shape of the LCO boundary looks double dip and LCO amplitude discontinuously increased as dynamic pressure increases after LCO onset. Hysteresis of LCO boundary was observed. Comprehension of these LCO behavior is necessary in development of SST with active control for aeroelasticity.

1 INTRODUCTION

Previous research on aeroelasticity of Supersonic Transport indicated some interesting phenomena. In the wind tunnel test of jet-powered supersonic experimental model, deep transonic dip was observed and divergent flutter existed over LCO region (Figure 1). The model was 11% scaled model of the NEXST-2 (National Experimental Airplane for Supersonic Transport) project, which has been canceled unfortunately. It had relative large engine nacelle and its effect has not been cleared. In a flutter test of a scaled model of silent supersonic transport, flutter speed reduction from a linear analysis was observed at Mach 0.90 and 1.02 (Figure 2). Around Mach 1.02, sharp drop of flutter speed was observed in narrow Mach range. Instabilities observed in those tests were LCO. SST must exceed transonic region where aeroelastic design is most critical. Further investigation of a behavior of LCO may enable to apply an active control. The wing model to endure to be exposed by LCO condition was made and wind tunnel test was performed in this study.

Figure 1: A wind tunnel model of jet powered experimental SST and its flutter boundary [1]

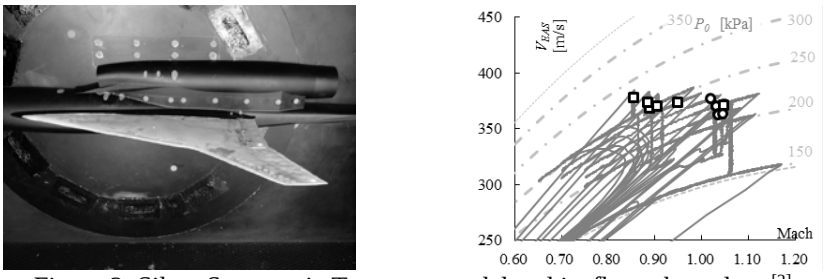

Figure 2: Silent Supersonic Transport model and its flutter boundary [2]

2 TEST FACILITY AND WING MODEL

2.1 Test facility

The flutter test was performed at transonic Flutter Wind Tunnel (FWT) in JAXA (Figure 3, Table 1). It is blow down type and duration time of a typical test is about 60 seconds. It has 60cm×60cm test section and a half model can be inserted and ejected by retractable system during the wind blows. Model retractable system is driven by pneumatic. It is aimed to avoid starting load on the model and to prevent from a model destruction. Flow condition can be changed in a certain rate to detect a flutter onset. So called Mach sweep is a flow sequence to change Mach number in a constant rate with constant total pressure, P_0. Mach change rate can be changed three steps in one operation. P_0 sweep sequence changes P_0 at constant Mach number. Dynamic pressure sweep sequence changes a dynamic pressure in proportion to Mach number. Mach sweep and P_0 sweep sequences were used in this test campaign.

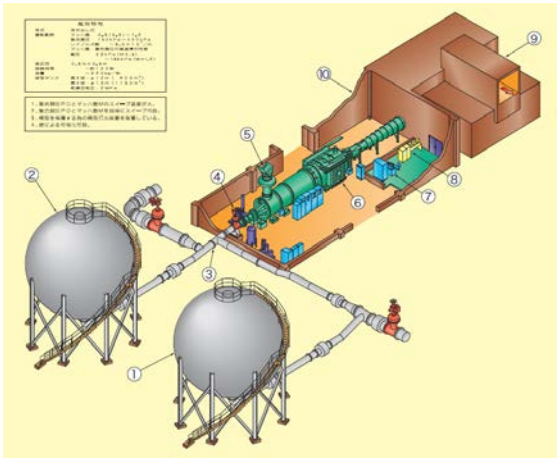

Figure 3 : Transonic Flutter Wind Tunnel (FWT)

Mach	0.54-1.15
total pressure	150-400kPa
Re	-6x10^6/0.1m
duration	-100 sec
operational sweep mode	Mach, P_0, Dynamics pressure

Table 1: Specification of FWT

2.2 Wing model

A planform of the wing model is based on the small supersonic transport of JAXA's research project[3] (Figure 4). A wing profile is NACA0003, which is not based on the model. It is planar wing and warp shape is not based on the model. Simple structure of metal was preferred for the model to endure a longer exposure to LCO condition. Material of the model is aluminum alloy and inboard surface was cut to reduce its stiffness. Cut area is shaped by clay. Lead was stuck by double-sided tape at the tip. It will be peeled if the amplitude of oscillation become large, avoiding from the model destruction. The model is connected to a block with two spars. The block is mounted to the retractable system. It has no body and has split plate at the root instead. The wing deformation was measured by a laser triangulator at the tip.

Eigen modes of the wing model analyzed by FEM are shown in Figure 5. Modes of the split plate are omitted. Although the structure is not simulated for any model, the mode shapes and relations of frequencies are reasonable comparing to the previous research models. Ground Vibration Test (GVT) was performed by the Multi-axis Vibration Evaluation System (MaVES) which consists of a robot arm and laser vibrometer. The frequencies of the GVT results are shown in Table 2.

A result of linear flutter analysis using Doublet Point Method (DPM)[4] is shown in Figure 6 and Figure 7. Predicted flutter speed is close to the operational limit of FWT.

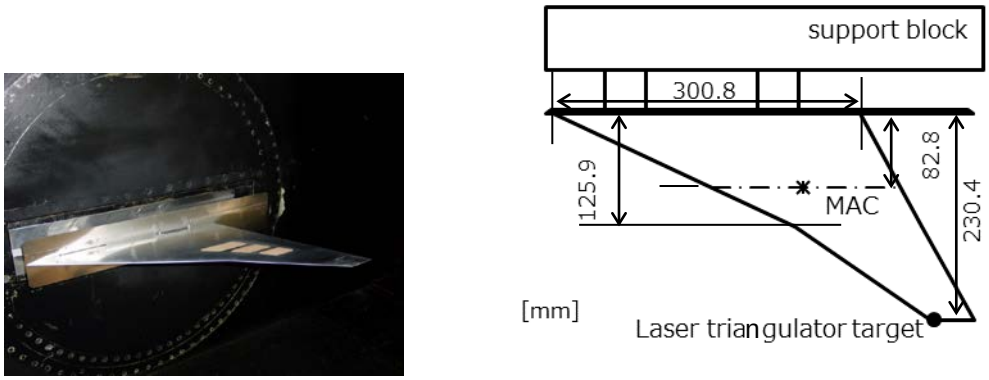

Figure 4: Wing model

#	mode	FEM Hz	GVT Hz
1	1st bending	65.7	64. 1
2	2nd bending	186.4	186.6
3	1st torsion	352.0	360.8
4	3rd bending	397.0	416.8

Table 2: Eigen mode frequencies

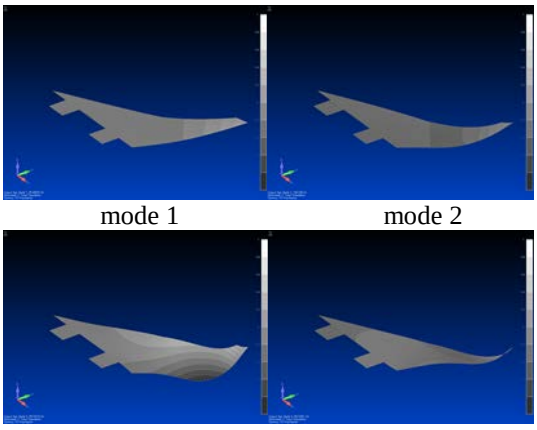

mode 1 mode 2

mode 3 mode 4

Figure 5: Mode shapes by FEM analysis

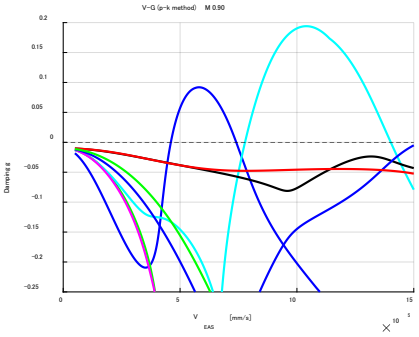

Figure 6: V-g chart by DPM at Mach 0.90

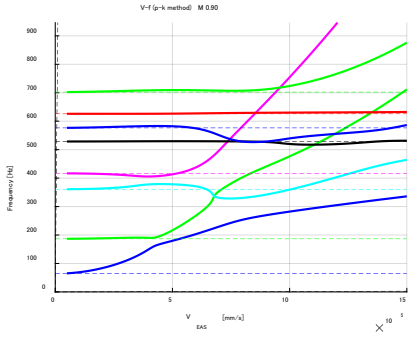

Figure 7: V-f chart by DPM at Mach 0.90

3 EXPERIMENTAL RESULTS

A boundary of the LCO observed in the experiment is shown in Figure 9. Initial angle of attack is 0 deg. The boundary is defined as the RMS of the oscillation of the deformation at the measured point reaches 1.2 or 1.5 mm and it is "stable". Stable means that the oscillation continues with the same amplitude. Filled marks show the large amplitude LCO which reaches 2.5 mm RMS. In the P0 sweep sequence, total pressure was increased at 1 to 3 kPa/sec. In the Mach sweep sequence, Mach number was changed at 0.003 to 0.004 /sec in both increasing and decreasing direction. In the Mach number decreasing process, the boundary is where the LCO stops. The LCO boundary shows double dip shape which has the bottom at Mach 0.94 and 1.01.

Variations of the RMS of deformation and frequency in P_0 sweep sequence at Mach 1.01 are shown in Figure 10. Numbers written in the figure mean run number of the wind tunnel test. Results of two test cases are shown in the Figure. As equivalent air speed (EAS) increased, the LCO started at 420 m/s. The equivalent air speed increased furthermore, the amplitude decreased. The EAS reached around 465 m/s, the amplitude jumped up to the larger condition. The frequency always increased as the EAS increased (Figure 11). As the EAS increased between 420 and 465 m/s, the vibration energy calculated by multiplication of the amplitude and the square of the frequency decreased. At some other Mach number close to the sonic speed, the similar phenomena were observed. Those cases are shown in Figure 12 and Figure 13.

Figure 14 shows RMS of deformation in Mach sweep sequence at P_0=360kPa. In run no. 15070, sweep rate is Mach 0.003/sec and in run no. 15073, it is Mach 0.010/sec. Difference of Mach sweep rate may bring the difference of the disturbance of flow. It seems to exist two equilibria and disturbance may change LCO amplitude.

Figure 15 and Figure 16 show RMS of the deformation in Mach sweep sequence. Each figure includes both increasing and decrease Mach sweep sequence. These figures show hysteresis of LCO in Mach wise direction. Mach sweep rate is thought small enough not to affect on the hysteresis. Existing of two equilibria is thought to be a reason.

Figure 17 shows RMS in P_0 sweep. P_0 was increased until 414 m/s EAS then it was decreased. The hysteresis of the LCO is also recognized in the P_0 sweep sequence.

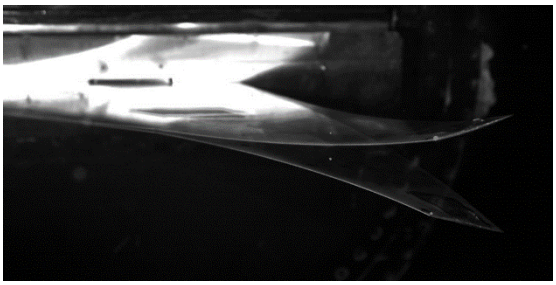

Figure 8: Superimpose image of high-speed camera at LCO

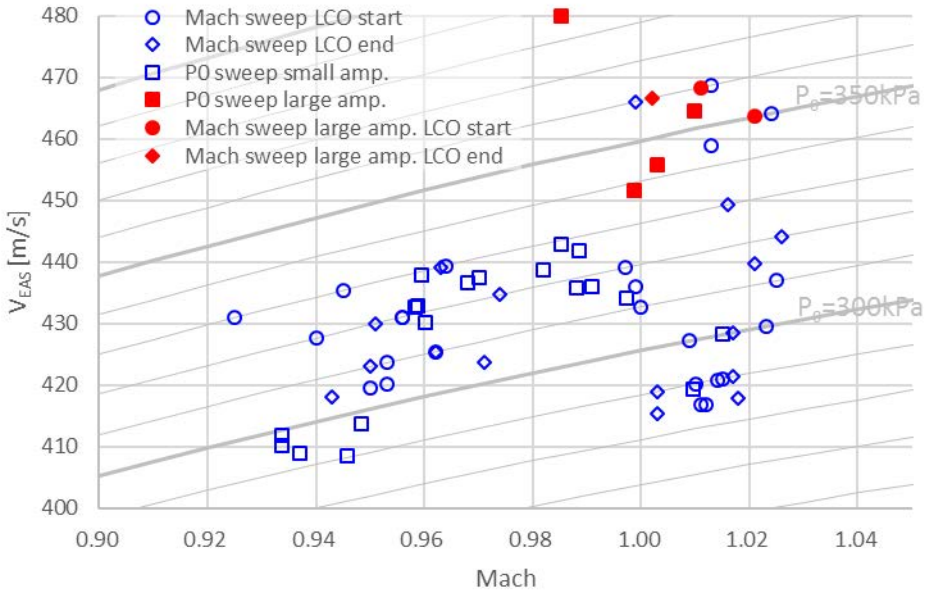

Figure 9: LCO boundary

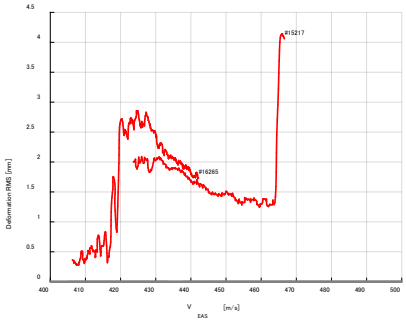

Figure 10: RMS variation at Mach 1.01

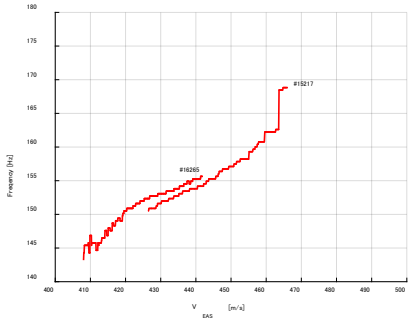

Figure 11: Frequency variation at Mach 1.01

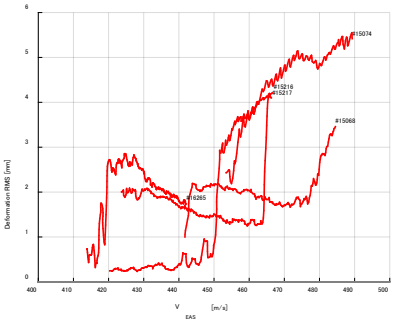

Figure 12: RMS variation

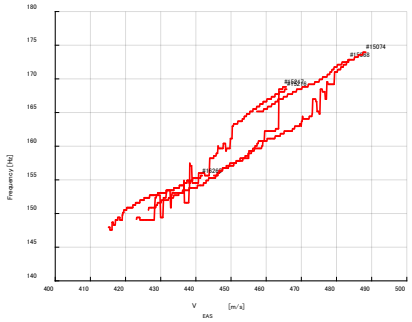

Figure 13: Frequency variation

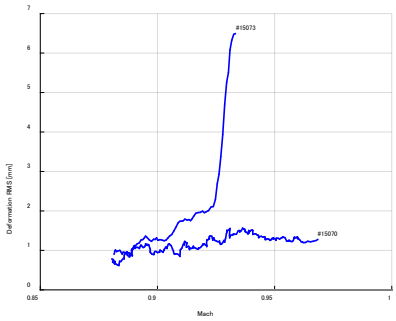

Figure 14: RMS in Mach sweep at different rate

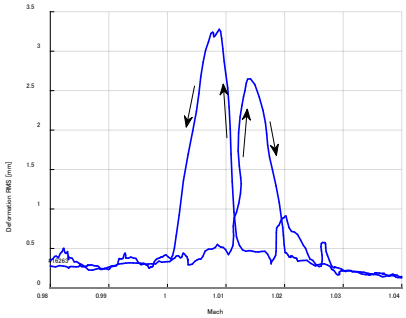

Figure 15: RMS in Mach sweep at P_0=285kPa

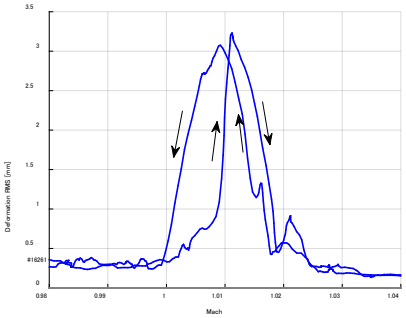

Figure 16: RMS in Mach sweep at P_0=290kPa

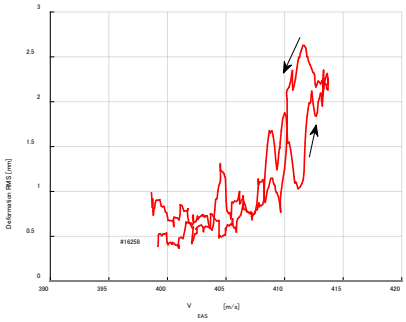

Figure 17: RMS in P_0 sweep at Mach

4 NUMERICAL ANALYSIS

Flutter analysis was performed with Euler code in addition to the DPM which is a linear aerodynamic code (Table 3). With the Euler code, generalized aerodynamics were calculated at some reduced frequency for three kinds of amplitudes (Figure 18) and p-k method was applied for eigen value analysis. Generalized aerodynamics of Euler code was obtained as simulation of forced oscillation was performed first, then the first harmonic component was derived. In the Euler analysis, only 4 modes were applied. In the DPM analysis, reducing the eigen mode reduces flutter speed in some extent. Although the flutter speed with Euler analysis is close to the DPM result, its frequency is much lower. Different amplitude of forced oscillation causes slightly difference of generalized aerodynamics and flutter speed. It needs more difference of flutter speed by the amplitude to explain the dip and LCO. Navier-Stokes analysis is thought to be necessary for it.

#	Unsteady aerodynamics	no. of modes	V_F m/s EAS	f_F Hz
	DPM	8	483.7	175.4
	DPM	4	469.8	170.5
	Euler amp. 0.005	4	455.0	108.1
	Euler amp. 0.100	4	469.4	111.9

Table 3: Analytical flutter speed at Mach 0.99

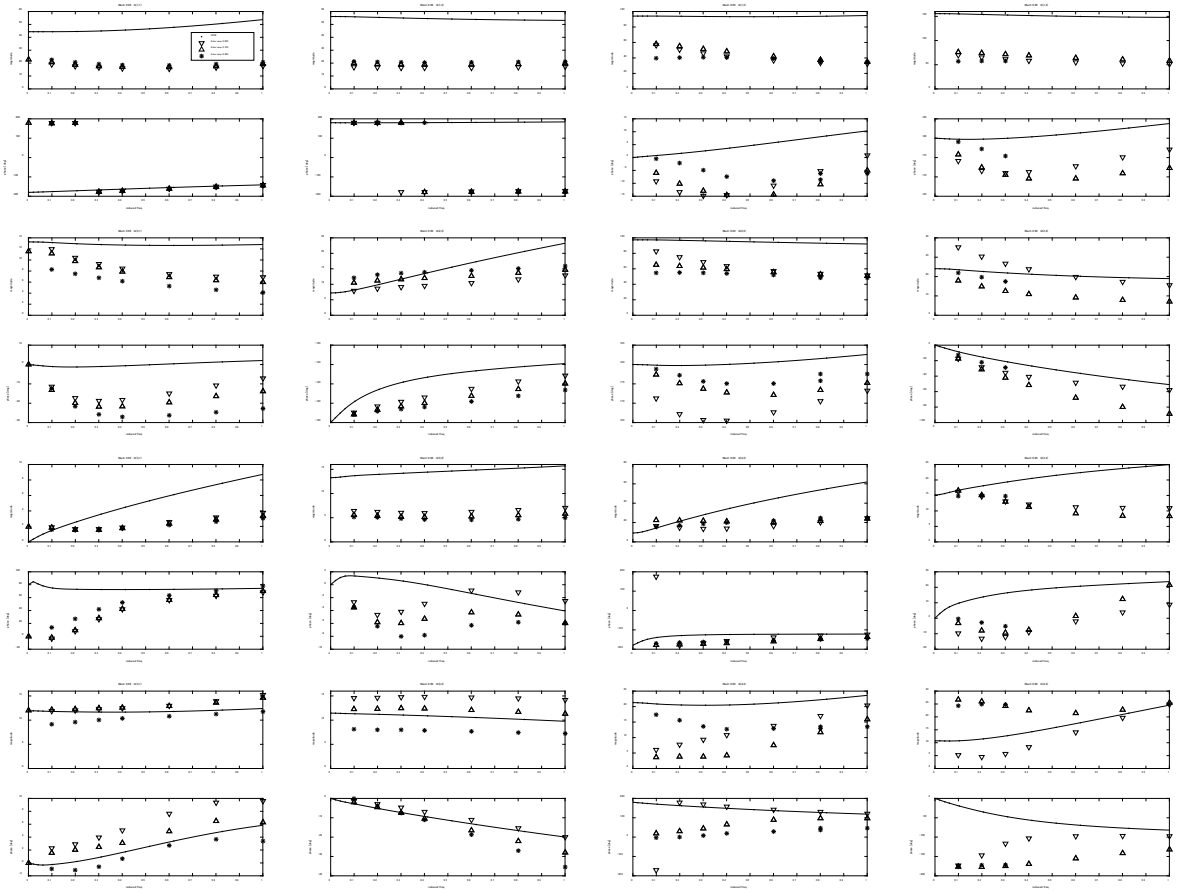

Figure 18: Generalized aerodynamics at Mach 0.99

5 CONCLUSIONS

Aeroelasticity of a cranked arrow wing for SST without engine nacelle was investigated. Following characteristics were observed in the wind tunnel test.

- Deterioration of the flutter speed in transonic region forms “double dip” which has the bottom at Mach 0.94 and 1.01.
- Increasing the dynamic pressure across the LCO region, amplitude of LCO become discontinuously enlarged.
- Two equilibria seem to exist and disturbance could shift the oscillation to larger amplitude.
- LCO region showed hysteresis by 1% both in Mach and P_0 sweep sequence.

Eigen value analysis for flutter with Euler code was performed. Navier-Stokes analysis seems to be necessary to explain the transonic dip and LCO.

6 REFERENCES

[1] Arizono, H., Machida, S., Kikuchi, T., Saitoh, K., Tamayama, M., Nakamichi, J., (2009) Experimental Transonic Flutter Results for Flexible Supersonic Transport Models. JAXA-RR-08-011 (in Japanese)

[2] Saitoh, K., Tamayama, M. and Yoshimoto, N., (2011) Flutter Characteristic of a Wing Model of the Silent SuperSonic Technology Demonstrator. JSASS-2011-3039 (in Japanese)

[3] Ueno, A. and Watanabe, Y. (2014) Multi-objective design optimization of nacelle layout for supersonic transport. JSASS-2014-5204 (in Japanese)

[4] Ueda, T. and Dowell, E. H. (1982) A New Solution Method for Lifting Surfaces in Subsonic Flow. AIAA Journal, vol. 20, No. 3, pp. 348-355

COPYRIGHT STATEMENT